SYNTHESIS AND CHARACTERIZATION OF Tb^{3+} ACTIVATED $Ba_3Si_6O_{12}N_2$ PHOSPHOR

S.A.Fartode[1], Anoop Fartode[2], S.J.Dhoble[3]
[1]Department of Physics, Dr.Babasaheb Ambedkar College of Engineering and Research, Nagpur
[2]Department of Chemistry, K.D.K. College of Engineering, Nagpur
[3]Department of Physics, RTM Nagpur University, Nagpur

Abstract

The nitride phosphors are useful for lighting application. Recently nitride phosphors has attracted interest because of its hardness, fracture strength , toughness, wear resistance, outstanding thermal and chemical stability, thermal resistivity, wide band gap and luminescent properties.

In this paper, synthesis and luminescent properties of Tb^{3+} activated $Ba_3Si_6O_{12}N_2$ oxinitride phosphor is reported. The material was synthesized through modified two step high temperature solid state diffusion technique. The prepared sample was confirmed by XRD technique. The Tb^{3+} activated $Ba_3Si_6O_{12}N_2$ material shows efficient blue green emission under 270nm excitation. The emission spectrum composed of two groups of lines in the wavelength range of 400-650nm. One group in the range 490-650nm corresponding to $^5D_4 \rightarrow {}^7F_J$ (J = 6,5,4,3) transitions of Tb^{3+} and other in range 400- 470nm originating from the $^5D_3 \rightarrow {}^7F_J$ (J = 6,5,4,3,2,1,0) transitions of Tb^{3+}. It is well known that Tb^{3+} concentration affects the relative intensities of $^5D_4$ and $^5D_3$ emissions of Tb^{3+} activated samples. The variation of Tb^{3+} concentration with intensity was also studied.

Keywords: $BaSi_2O_2N_2$; mechano luminescence;. phosphor; photo luminescence; solid state diffusion method;

I. Introduction

Inorganic phosphors are widely used in variety of applications such as lamp industry, X-ray imaging, scintillators and color display. Recently there has been a growing focus on research in the area of white light emitting diode due to their merits such as being environmental friendly, highly efficient and longer lifetime [1-3]. During past few years the white-LEDs fabricated using near-UV LEDs coupled with red, blue and green phosphor have attracted much attention. The current interest focuses on novel down-converting phosphors that can be effectively excited with near UV light. As far as the materials themselves are concerned, silicon oxynitride phosphors are very attractive because of their high efficiency [4,5], wide range of emission, chemical stability and good thermal quenching. Most importantly these phosphors emit visible light efficiently under near-ultraviolet or blue light irradiation allowing them to be used as down-conversion luminescent materials for white light-emitting diodes (LEDs).

In Tb^{3+} doped material the emission occurs in blue–green region. This occurs due to the transitions of $^5D_3$ and $^5D_4$ excited states to ^7F_J (J=0, 1,…, 6) ground states of Tb^{3+} ions. Under UV excitation the Tb^{3+} ions ($4f^8$) are raised to the higher $4f^75d^1$ level and then transferred to $^5D_3$ or $^5D_4$ excited states [6]. There is a wide applicability of Tb^{3+} activated phosphors such as projection television tubes, X-ray intensifying screens, three-band fluorescent lamps and various photonic applications [7].

The $Ba_3Si_6O_{12}N_2$:Eu^{2+} phosphor was prepared by liquid phase precursor method reported by Y.H.Song et al. [8] To the best of our knowledge the research has been carried out on the luminescence properties of Tb^{3+} doped

$Ba_3Si_6O_{12}N_2$ and its corresponding application in W-LEDs.

II. Experimental

$Ba_3Si_6O_{12}N_2:Tb^{3+}$ phosphors was synthesized by high temperature solid-state diffusion method. The starting materials were high purity $BaCO_3$ (Merck, >99.0%), α-Si_3N_4 powder, Tb_2O_3 of AR grade. The appropriate amount of starting materials were weighed out separately on an analytical balance and subsequently mixed and ground together in an agate mortar. The powder mixtures were then transferred into crucibles and fired in a furnace at 400^0C for 1 hr. Then these mixtures were crushed in an agate mortar for one hour and fired in a horizontal tube furnace (muffle furnace) at 800 ^{0}C for 24 hour in charcoal atmosphere. The samples were gradually cooled to room temperature in a furnace. Finally the samples were quenched at 1200^0 C in same atmosphere and pulverized for further measurements. All measurements were performed on finely ground samples which were analyzed by X-ray powder diffraction. All the XRD measurements were performed at room temperature in air. The composition and phase purity of products were measured by powder X-ray diffraction (XRD) analysis with an X'Pert PRO diffractometer with Cu-Kα radiation (λ= 1.54060Å) operated at 45 kV and 40 mA. The XRD data were collected in a 2θ range from 10^o to 80^o. The photoluminescence (PL) emission spectra of the sample were recorded using spectrofluorophotometer (shimadzu RF-5301). The same amount of sample was used in each case. The emission and excitation spectra were recorded using spectral slit width of 1.5 nm. SEM micrographs were carried out using a HITACHI S-4800 scanning electron microscope. The SEM micrographs were taken at 5000 V accelerating voltage, 8300 µm working distance,7800 nA emission current at high lens mode with fast scan speed and gray scale color mode.

III. Results and discussion

A. X-ray diffraction, Crystal Structure & Scanning Electron Microscopy

The XRD pattern of the sample was analyzed for structure confirmation. Fig. 1 represents the powder XRD pattern of $Ba_3Si_6O_{12}N_2$ prepared by solid diffusion technique. XRD pattern of prepared material matched with XRD pattern reported by Y.H.Song et al. [8], but the sample show some unknown phases. If the heat treatment would have been given to the sample the unknown phases might have disappeared. Fig. 2 represents the crystal structure of $Ba_3Si_6O_{12}N_2$ which crystallized as a trigonal structure (adopted from the work of Y.H. Song et al. with P-3 space group (no.147)). The reported lattice constants were a = 7.5046 Å and c = 6.4703Å. $Ba_3Si_6O_{12}N_2$ consists of corrugated layers of vertex-sharing SiO_3N tetrahedrons between Ba^{2+} ions. Two different trigonal antiprism sites were occupied by two Ba^{2+} ions. In the $Ba_3Si_6O_{12}N_2$ lattice the oxygen atoms are coordinated with one Ba^{2+} ion to form a distorted octahedron while six oxygen atoms and one nitrogen atom is coordinated with another Ba^{2+} ion. [8].

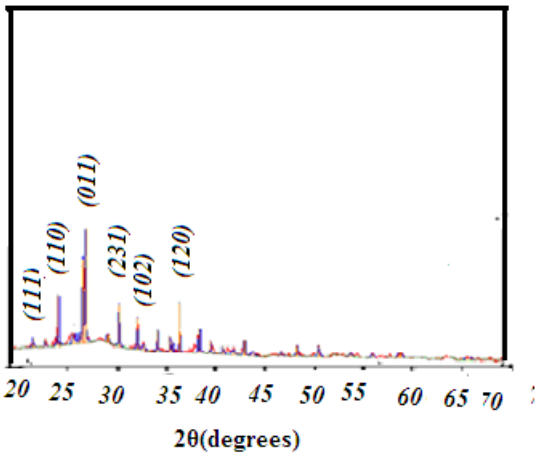

Fig.1 XRD of $Ba_3Si_6O_{12}N_2$

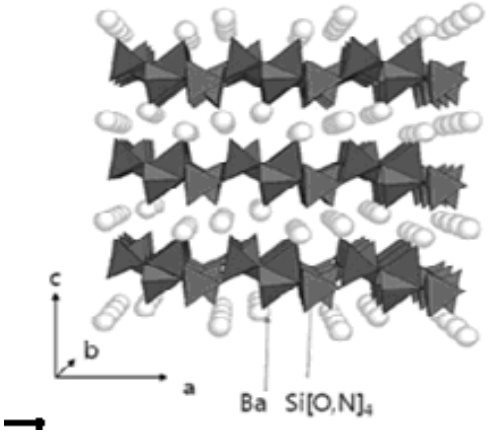

Fig.2 Crystal structure of $Ba_3Si_6O_{12}N_2$

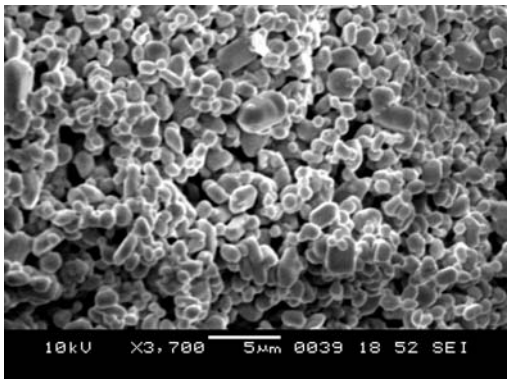

Fig.3 Morphological image of $Ba_3Si_6O_{12}N_2$:Eu^{2+} phosphor

The surface morphology of the microcrystalline nitride was examined by scanning electron microscopy (SEM, JEOL 6380 A). The typical morphological image is represented in Fig. 3. When the phosphor was prepared at high temperature the particles growth took place rapidly forming bigger particles. The average particle size increased to around 5µm as can be seen in SEM images.

B. Luminescence of $Ba_3Si_6O_{12}N_2$:Tb^{3+}

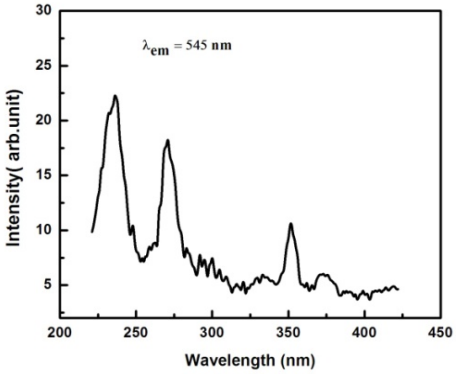

Fig.4 Excitation spectrum of $Ba_3Si_6O_{12}N_2$:Tb^{3+} phosphors

The several peaks are obtained in excitation spectra between 200 nm to 400 nm. The excitation peaks at 280–393 nm may be caused by 4f-4f transitions of Tb^{3+} ions [9]. This clearly indicates that the phosphors can be effectively excited by UV. The excitation spectrum was obtained by monitoring the $^5D_4 \rightarrow {}^7F_5$ transition of Tb^{3+} at 545 nm and is shown in Fig.4.

An excitation band with maximum at 240 nm result from the lowest spin allowed f-d transition. The band corresponding to the first spin forbidden f-d transition is very weak between 300 nm and 500 nm. These bands can be attributed to spin forbidden transitions within 4f shell of Tb^{3+}. The emission peak for all concentrations are same and resulting from $^5D_4 \rightarrow {}^7F_5$ transition of Tb^{3+}. The efficient shielding of 4f orbital from fully occupied 5s and 5p orbital resulted in no shift of position of the peaks which corresponds to the f-f transitions.

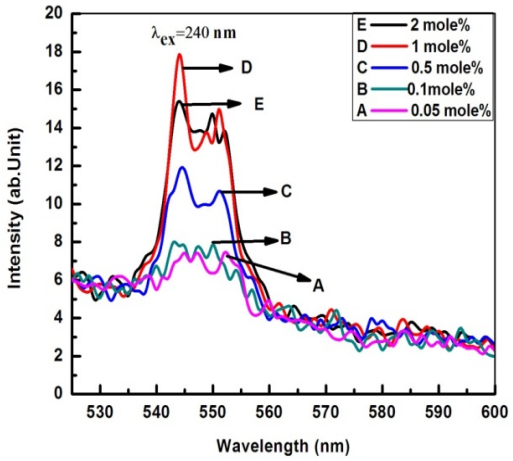

Fig.5 Emission spectra of $Ba_3Si_6O_{12}N_2$:Tb^{3+} phosphors when excited at 240 nm.

The strongest emission peak is located at 543 nm which is responsible for green emission (Fig.5). The emission peak caused by $^5D_4 \rightarrow {}^7F_5$ transition is split into two peaks (543 and 552 nm). These splits are related to crystal field effect [10]. A similar result was reported in case of $La_{1-x}AlO_3$:xTb^{3+} phosphors studied by S.J. Yoon et al. [9] They reported that under 256 nm excitation the emission spectrum of $La_{1-x}AlO_3$:xTb^{3+} phosphors showed two major emission peaks at 543 nm and 582 nm which were attributed to $^5D_4 \rightarrow {}^7F_5$ and $^5D_4 \rightarrow {}^7F_4$ transitions of Tb^{3+} ions respectively. The emission peak due to $^5D_4 \rightarrow {}^7F_5$ is split into 543 and 550 nm peaks and emission peak due to $^5D_4 \rightarrow {}^7F_5$ is split into 582 and 589 nm peaks. It is well known that the concentration of Tb^{3+} ions affect the emission intensity. The emission intensities centered at 543 nm as a function of Tb^{3+} content are shown in Fig.6.

The emission intensity increases with Tb^{3+} content up to x = 1mole% due to energy transfer between host and dopant and then decreases with the further increase of Tb^{3+} content due

to the energy transfer between the neighboring Tb^{3+} ions *i.e.* quenching of the emission of Tb^{3+} ions [11]. The non radiative energy transfer may occur due to an exchange interaction, radiation reabsorption or electric multipolar interactions [12].

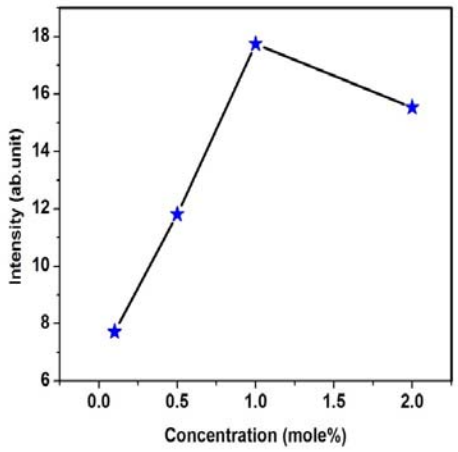

Fig. 6 Emission intensities centered at 545 nm for the $Ba_3Si_6O_{12}N_2$:Tb^{3+} (0.05≤x≤2) phosphors

The investigation of non-radiative energy transfer is important for the basic understanding of the physical excitation processes [13]. The quantitative theories for non-radiative energy transfer were proposed by G. Blasse [14]. The concentration quenching may occurs due to migration of excitation energy from one activator center to another and ultimately to an imperfection which may act as energy sink. The dependence of fluorescence yield on concentration and typical activator concentrations at which appreciable quenching may be expected to occur were explained by Dexter and Schulman [15].

IV. Conclusion

In the present work $Ba_3Si_6O_{12}N_8$:Tb^{3+} was synthesized by high temperature modified solid state diffusion method. The luminescence properties of Tb^{3+} in $Ba_3Si_6O_{12}N_2$ material were investigated. It shows the green emission peaks at 543 nm at 240nm excitation for Tb^{3+} ion. In the excitation spectra of Tb^{3+} several sharp peaks (200–400 nm) were observed. The emission intensity of Tb^{3+} doped $Ba_3Si_6O_{12}N_2$ phosphors increased with increasing Tb^{3+} content and the maximum intensity was obtained at x= 1 mole%. . The surface morphology shows that the size of particle was around 5μm.

V. References:

[1] W. B. Im, Y. I. Kim, N. N. Fellows, H. Masui, G. A. Hirata, S. P. DenBaars, and R.Seshadri, Appl. Phys. Lett. 93(9) (2008) 091905.

[2] T. Nishida, T. Ban, and N. Kobayashi, Appl. Phys. Lett 82(22) (2003) 3817.

[3] J.S.Kim, P.E.Jeon, J.C.Choi, H.L.Park, S.I.Mho and G.C.Kim, Appl. Phys.Lett., 84(2004) 2931.

[4] C. J. Duan,W. M. Otten, A.C.A. Delsing and H.T. Hintzen, J. Alloys and Compds, 461(2008) 454.

[5] T. Suehiro, N. Hirosaki, R. Xie, K. Sakuma, M. Mitomo, M. Ibukiyama and S. Yamada, Appl. Phys. Lett., 92(19) (2008) 191904.

[6] J.Y. Park, H.C. Jung, G.S.R. Raju, B.K. Moon, J.H. Jeong and J.H. Kim, J.Lumin, 130 (2010) 478.

[7] S.P. Khatkar, S.D. Han, V.B. Taxak, G. Sharma and D. Kumar, Opt. Mater., 29 (2007)1362.

[8] Y.H. Song , M.O. Kim , M.K. Jung , K. Senthil and T. Masaki, K. Mater. Lett., 77(2012)121. J. Lumin. 130 (2010) 678.

[9] S.J. Yoon, S.J. Dhoble and K. Park, Ceramics International 40 (2014) 4345.

[10] P. Li, L. Pang, Z. Wang, Z. Yang, Q. Guo and X. Li, J. Alloys and Compds 478 (2009) 813.

[11] M. Weng, R. Yang, Y. Peng and J. Chen, Ceramics International 38 (2012)1319.

[12] L. Jiang, C. Chang, D. Mao, and C. Feng, Mater. Sci. and Eng B,103 (2003) 271.

[13] J. Zhang, Y. Wang, Z. Zhang, Z. Wang and B. Liu, Mater. Lett., 62 (2008) 202.

[14] G. Blasse Phys Lett. A, 28 (1968) 444.

[15] D.L. Dexter and J.H. Schulman, J. Chemical Physics, 22 (1954) 1063.